Proceedings of ASME Turbo Expo 2011
GT2011
June 6-10, 2011, Vancouver, British Columbia, Canada

GT2011-45881

EXPERIMENTAL DETERMINATION OF FLAME TRANSFER FUNCTION USING RANDOM VELOCITY PERTURBATIONS

Alexis Cuquel[*]**, Daniel Durox, Thierry Schuller**
Laboratoire EM2C - Ecole Centrale Paris - CNRS
Grande Voie des Vignes, 92295 Châtenay-Malabry, France
Email: alexis.cuquel@em2c.ecp.fr

ABSTRACT

This study focus on the experimental determination of the Flame Transfer Function (FTF) which can be used to analyze acoustic induced combustion instabilities. In the present work random non-harmonic velocity signals are generated to perturb the flame. This method enables to rapidly determine the FTF compared to other techniques and improves the frequency resolution. A System Identification (SI) technique is applied to model the frequency response of different components of the test bench. It is firstly used to impose a white noise velocity signal at the burner exit, with a tunable perturbation level. SI tools and spectral analysis are used to reconstruct the FTF of a laminar conical flame. Experiments are conducted for different operating conditions and forcing levels. Results are compared with those obtained by harmonic modulations of the flow. They closely match over a large frequency range for small perturbation levels. The limits of the technique are examined when the modulation amplitude is increased.

NOMENCLATURE

FTF Flame Transfer Function
G Gain of the FTF
φ Phase of the FTF
v' Velocity perturbation
$\dot{Q}'$ Heat release rate perturbation
FDF Flame Describing Function
SI System Identification
FIR Finite Impulse Response
IIR Infinite Impulse Response
LDV Laser Doppler Velocimetry
PSD Power Spectral Density

INTRODUCTION

Acoustic induced combustion instabilities are generated by a strong coupling between the flame dynamics and the burner acoustics [1]. They generally take the form of a limit cycle characterized by a certain oscillation frequency and amplitude reached by the flow variables within the combustor. Prediction of these unstable modes and their corresponding oscillation amplitudes are important to capture the overall effects of these instabilities on the combustion chamber. As different efficient methods were developed to determine the frequency response of the combustor and the corresponding eigenmodes [2–4], research is mainly focused on flame dynamics. Early work in rocket engine instabilities established a link between pressure and the heat release rate fluctuations through a simple model. Those two quantities were linked by an interaction index n and a time delay τ, leading to the well-known $n-\tau$ model [5].

To gain more insight into the mechanisms governing the flame dynamics under self-sustained oscillations, the frequency response of the flame submitted to imposed flow rate or mixture composition fluctuations can be examined. The Flame Transfer Function, linking these flow perturbations to the resulting heat release rate fluctuations, has been proven to be a reliable tool to predict the occurence of thermo-acoustic instabilities in generic or practical configurations. It is usually expressed in terms of a gain G and a phase φ which define the ability of the flame dy-

[*]Address all correspondence to this author.

namics to positively feed energy back into the burner acoustics as a function of the modulation frequency. This response can be determined theoretically [6–8] or numerically [9] in a few cases, but in many applications, an experimental determination of the FTF is required [10–12]. Although mixture composition oscillations were shown to be an important phenomenon to take into account [13, 14], only the response of flames submitted to velocity perturbations are considered in the following. The methodology developed in this study is tested and validated in a generic configuration corresponding to a laminar conical flame.

Theoretical and experimental analysis of the response of premixed laminar conical flames have shown that the FTF strongly depends on the perturbation frequency. In [15, 16], it is shown that this flame acts as a low-pass filter, meaning that the gain vanishes for large frequencies, whereas a unity gain is found at low forcing frequency [6, 7, 17, 18]. Experiments have pointed out a linear increase of the phase φ of the FTF as the forcing frequency is increased [7, 19, 20], which can be captured by including the convective nature of the velocity field [8,9,21,22]. Recent work also clearly indicates that the gain is decreasing [23] and the phase slope is changing [24, 25] when the perturbation level increases. This in turn may modify the combustor stability because the flow disturbances level and phase lag with respect to heat release rate oscillations change. To take into account this amplitude dependent response, a Flame Describing Function (FDF) concept can be introduced [26] which describes the flame response as a function of the frequency and input level. The FTF from a laminar conical flame is thus very sensitive to slight variations of the perturbation frequency and disturbance level. It constitutes a good configuration to test and validate different experimental methodologies to determine the FTF.

The FTF is generally determined by imposing harmonic velocity modulations characterized by Laser Doppler Velocimetry (LDV), two-microphones technique or hot wire probe anemometry. A photodiode enables to determine the resulting heat release rate fluctuations [10–12]. These signals are gathered and post processed by calculating the cross- and auto-power spectra to obtain the FTF. The same type of procedure can be used to determine the FDF based on harmonic incoming velocity signals, but the level of excitation should be kept constant over the forcing frequency range. The measurements are then repeated to obtain a set of FTF at different forcing levels.

Lately, new ways to determine Transfer Functions in aeroacoustics have been used to determine this frequency response with numerical simulations. Following the theory of System Identification (SI, see [27] for an extensive description), these methods require the use of broadband or impulse signals to perturb the system (Fig. 1). The time series data of velocity and heat release rate can then be used to retrieve the coefficient of a filter approximating the FTF. In [3], the auto- and cross-correlation matrices have been numerically computed and the inversion of the Wiener-Hopf equation was performed :

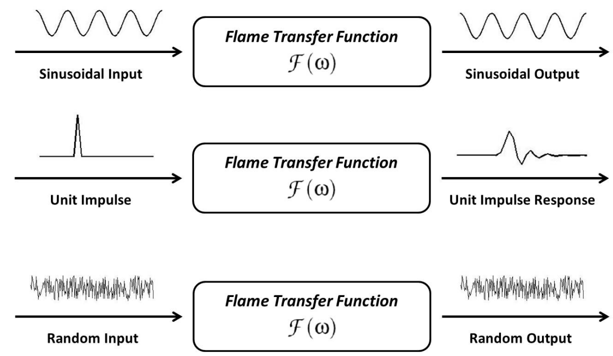

Figure 1. Different input signals can be used to determine the FTF, such as harmonic signals, unit impulse or random signals.

$$\Gamma h = c \tag{1}$$

where Γ is the auto-correlation matrix of the velocity signal and c is the cross-correlation matrix of the heat release rate perturbation and the velocity perturbation signals. This leads to the unit impulse response h of the system, which z-transform is the acoustic transfer function approximated as a Finite Impulse Response (FIR) filter. The same tools [28] were used, but coupled to several broadband noisy signals to modulate the flame and retrieve the FTF with a good accuracy except in the low frequency range. A space-dependent FTF was numerically approximated in [29] using a sum of random-phase sinusoids to modulate the flow and an Infinite Impulse Response (IIR) filter using an autoregressive exogeneous model to compute the filter coefficients.

In the present work, these alternative methods are tested to determine the FTF of a conical flame. It is shown that random velocity perturbations can be used instead of harmonic signals to obtain results with a better frequency resolution in a shorter time. The theoretical framework of determination is explained. Spectral analysis is first used to compare results obtained with harmonic and random velocity perturbations. The SI tools are then used to retrieve the coefficents approximating the FTF as an IIR filter. After a description of the experimental setup, a procedure to control the velocity forcing signal at the burner nozzle outlet will be detailed. This method enables to use a nearly white noise signal as the forcing input. FTF determined with this forcing signal will be compared to that obtained using classic harmonic velocity modulations. Effects of the input level are then examined together with a sensivity analysis based on the sampling time and the number of coefficients used to built the filter that models the burner response.

1 FLAME TRANSFER FUNCTION DETERMINATION

The FTF is computed from the gathered time series of the input signal, namely the velocity perturbation at the flame base, and the output signal corresponding to the heat release rate perturbations measured by a photomultiplier. The type of forcing signal is an important aspect of the methodology and can take different forms. Two kinds of forcing signal are tested here.

To analyse the flame response in the Fourier space, a set of harmonic velocity perturbations $v'(t)$ can be used at different forcing frequencies. These signals are defined by an amplitude $\tilde{v}$ and a real angular frequency ω so that $v'(t) = \Re\{\tilde{v}e^{-i\omega t}\}$ where $\Re$, $\tilde{v}$ and ω respectively stands for the real part of a complex number, the amplitude and the angular frequency of the perturbation.

However, the measurement process, by sweeping frequencies over the range of interest, is fairly long and can be improved. Multi-tone signals have been proposed as alternative techniques to excite the flame. Imposing random multi-tone velocity perturbations enables to modulate the flame over a large frequency range. This can be used to obtain the whole FTF at once, but also to increase the frequency resolution of the FTF. In the following, a white noise signal will be used as a random multi-tone signal, which is defined by:

$$v'(t) = \tilde{v}.rand_{[-1,1]} \tag{2}$$

where $\tilde{v}$ is the perturbation amplitude and $rand_{[-1,1]}$ stands for a random number generator which results are statistically uniformly or normally distributed over the interval [-1,1]. The use of a white noise signal here enables to excite the flame with an equally distributed power over a large range of frequencies. This has already been used in numerical simulations but raises some experimental difficulties which must be overcome as further described in this study.

The FTF gain G and phase φ are then computed, at a particular forcing angular frequency ω for a harmonic modulation using the auto- and cross-power spectral densities of the velocity and heat release rate signals:

$$\mathcal{F}(\omega) = \frac{S_{v',\dot{Q}'}(\omega)}{S_{v',v'}(\omega)} = G(\omega)e^{i\varphi(\omega)} \tag{3}$$

This method has been widely used to compute FTF. For random modulations, post-processing techniques were also developed to compute the FTF. Cross-power spectral density analysis is a natural choice to examine the response. The use of a random input signal enables to determine the FTF over a wide frequency range and the auto and cross-power spectral densities of the input v' and output $\dot{Q}'$ signals can still be computed. Long windowed time series along with averaging techniques are needed to reach statistical convergence :

$$\mathcal{F}(\omega) = \frac{1}{N}\sum_{k=1}^{N} \frac{S^k_{v',\dot{Q}'}(\omega)}{S^k_{v',v'}(\omega)} \tag{4}$$

where N is the number of time series which has been collected.

SI methods can also been used to compute a linear FTF from time series of the input (incoming velocity perturbations) and output (heat release rate perturbations) signals. The IIR method is used in the following to determine the system impulse response. This impulse response $h(t)$ completely defines a linear process :

$$\dot{Q}'(t) = \int_{-\infty}^{+\infty} h(\tau)v'(t-\tau)d\tau \tag{5}$$

where $v(t)$ and $\dot{Q}'(t)$ are the input and output signals of the process. This equation can be approximated in a discrete form by:

$$\begin{aligned}\dot{Q}'_n + a_1\dot{Q}'_{n-1} + ... + a_{n_a}\dot{Q}'_{n-n_a} \\ = b_0 v'_n + b_1 v'_{n-1} + ... + b_{n_b} v'_{n-n_b} + e(t)\end{aligned}$$

where v'_i and $\dot{Q}'_i$ are the sampled input and output signals, a_i and b_i stand for the reverse and forward coefficients, n_a and n_b define the order of the model and e(t) the noise disturbance. A sufficient number of coefficients n_a and n_b has to be chosen to take account of the largest time lag involved in the system. This point will be further examined for the FTF determination. This leads to an approximation of the FTF as an IIR filter of the form :

$$\mathcal{F}(\omega) = \frac{\sum_{k=0}^{n_b} b_k z^{-k}}{\sum_{k=0}^{n_a} a_k z^{-k}} \tag{6}$$

where $z = \exp(i\omega)$.

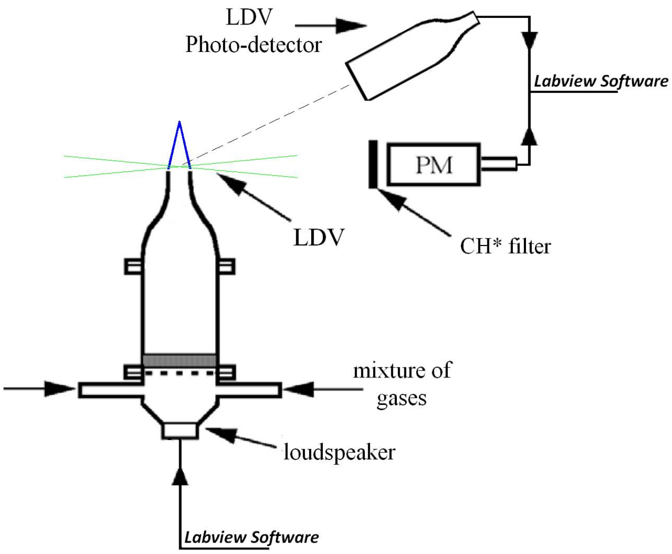

Figure 2. Experimental setup for FTF determination.

2 EXPERIMENTAL CONFIGURATION

The configuration studied here is presented in Fig. 2. It features a cylindrical feeding manifold equiped with a laminarization grid and a convergent nozzle used to reduce remaining turbulent fluctuations and to get a nearly uniform top-hat velocity profile at the burner exit. This burner exit is circular, of radius $R = 11$ mm. The bottom of the burner is also equipped with a loudspeaker to impose harmonic or random velocity perturbations in the feeding manifold and at the base of the flame. By changing the mixture flow rate, the mean bulk velocity at the burner exit can be imposed. The CH4-air mixture is perfectly premixed before entering the manifold and was fixed to an equivalence ratio $\phi = 1.03$, which sets the laminar burning velocity to $S_L = 0.39$ m.s^{-1}.

The loudspeaker signal input, velocity and heat realease rate time series are all recorded with a National Instrument analog-to-digital converter board controlled by the Labview software. The sample frequency is 4096 Hz. The velocity signal is measured by LDV at the base of the flame, 2 mm above the burner exit on the burner axis. A photodiode (PM) equipped with an OH* filter is used to collect the chemiluminescence emission from the flame, which is proportional to the heat release rate [30]. The Labview software is also used to post-process these data, and to generate the forcing signal with a sample frequency of 4096 Hz. This signal is sent to an amplifier which drives the loudspeaker (Fig. 3). An home-made Labview program was developed to enable an easy sweep of the perturbation frequency and amplitude. Different filters are also used to control the flow perturbation produced at the burner exit. This last point is detailled in the next section.

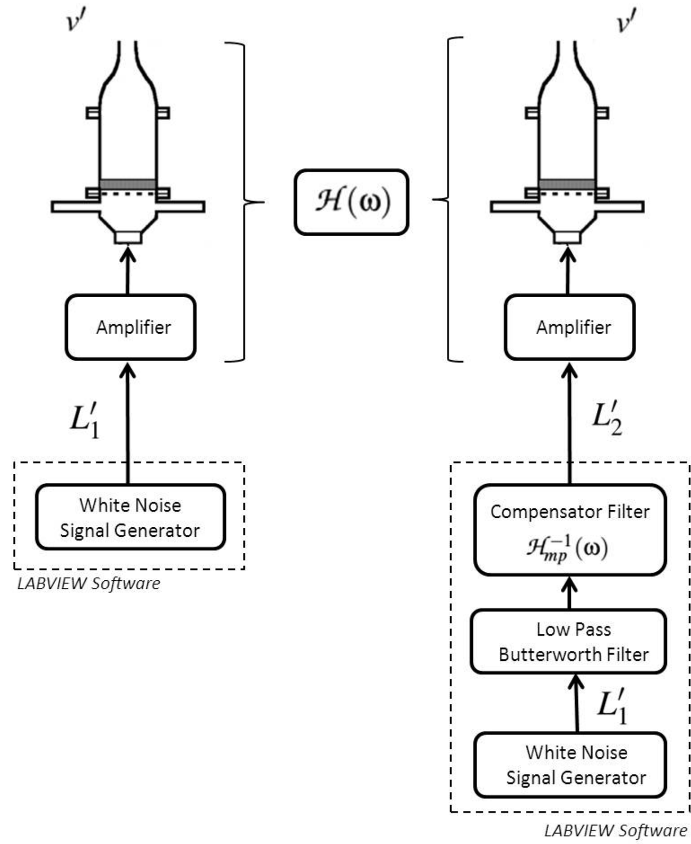

Figure 3. Scheme of the system set up to obtain uncontrolled (leftside) and controlled (rightside) flow modulations v' at the burner exit.

Loudspeaker, amplifier and burner Transfer Function

The white noise signal generated with the Labview software is sent to an amplifier followed by a loudspeaker to modulate the flow in the burner cavity. Preliminary experiments were focused on characterizing the resulting velocity pertubation signal at the burner exit. When the flow is acoustically forced with a harmonic signal, the flow is also responding harmonically as expected. In this case, the amplitude of the velocity modulation can be measured by LDV and tuned to keep the same forcing level for each frequency investigated. When random broadband velocity fluctuations are synthesized, the situation is different. The response can be first characterized by plotting the velocity power spectrum at the burner outlet and compared with the power spectrum generated by the signal generator (Fig. 4a).

This figure indicates a significant difference between the perturbation level of the resulting velocity modulations over the frequency range of interest. This signal does not correspond to white noise but features a colored spectrum. This is due to the combined responses of the loudspeaker, amplifier and burner which filter the perturbations and can be characterized by a trans-

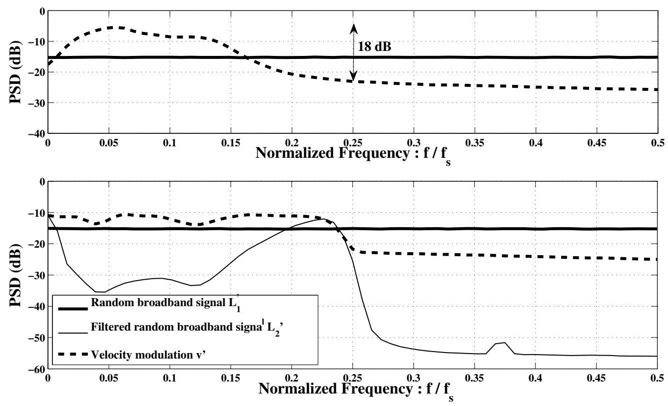

Figure 4. Power Spectral Densities of a) (—) the random broadband signal L_1' and (- - -) the uncontrolled velocity perturbation v' b) (—) the random broadband signal L_1', (...) the filtered broadband signal L_2' and (- - -) the controlled velocity perturbation v'. The Nyquist frequency, f_s, is here equal to 2048 Hz.

fer function $\mathcal{H}(\omega)$ (Fig. 4a)) that must be determined.

SI tools are then firstly used to characterize the transfer function $\mathcal{H}(\omega)$ of the elements formed by the amplifier, the loudspeaker and the burner. By using a white noise signal generated with the Labview software and gathering the induced velocity time serie at the burner exit, it is possible to determine the transfer function $\mathcal{H}(\omega)$ defined as follows :

$$\mathcal{H}(\omega) = \frac{v'/\bar{v}}{L_1'} \tag{7}$$

where L' stands for the Labview-generated white noise signal used as an input to the amplifier. A total of $n_a = 50$ and $n_b = 50$ filter coefficients were used to reach a good estimation of $\mathcal{H}(\omega)$. As shown in Fig. 4a, this frequency response features a pass band filter where frequencies under 80 Hz and above 200 Hz are greatly damped. A correction needs to be applied to compensate the effect of the amplifier and the loudspeaker in the Fourier space.

To obtain a white noise velocity signal at the burner outlet, the inverse transfer function $\mathcal{H}^{-1}(\omega)$ was first applied to the Labview white noise signal. The resulting signal clearly showed that $\mathcal{H}^{-1}(\omega)$ was unstable - some of its zeros were out of the unit circle -. To cope with that issue, we choose to compute the minimum-phase inverse transfer function $\mathcal{H}_{mp}^{-1}(\omega)$ which is a stable transfer function that has the same exact gain as $\mathcal{H}^{-1}(\omega)$ but a different phase (see [31] for details). As we are here dealing with random phase signals, inverting the magnitude of $\mathcal{H}(\omega)$ to obtain a nearly-white-noise velocity signal is essential whereas

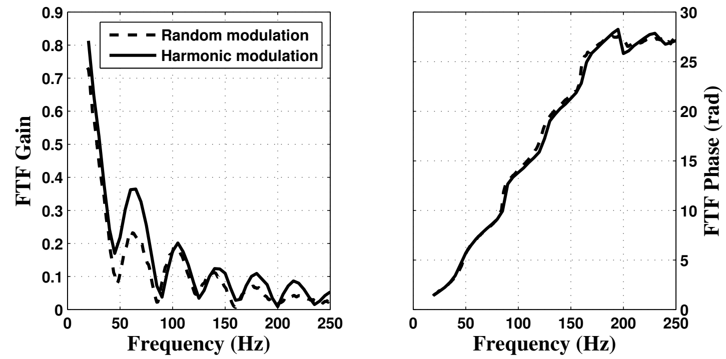

Figure 5. FTF obtained through harmonic and random velocity modulation and cross-correlation techniques, for a relative rms velocity perturbation of $v_{rms}/\bar{v} = 0.04$.

the phase of the resulting velocity signal is of less importance. This new filter $\mathcal{H}_{mp}^{-1}(\omega)$ features now a stable response with smooth transitions between frequencies but it still contains too high frequencies with significant power spectral densities. This can easily be removed by first applying a low pass filter.

We choose a 20^{th} order Butterworth filter with a cut-off frequency of 500 Hz. This provides an almost flat frequency response up to 500 Hz and removes the upper frequencies well above the cut-off frequency of the flame response. The PSD of the resulting velocity signal is shown in Fig. 4b. It exhibits a nearly uniform power density over the range of frequency of interest. The difference between the maximum and the minimum of the PSD is reduced to less than 5 dB, that can be compared to the 20 dB difference for a velocity signal generated without correction. This preprocessing procedure can now be used to generate random velocity fluctuations at the burner outlet and compare the flame response to that obtained for harmonic flow modulations.

3 RESULTS

The flame response are first examined for small amplitude velocity perturbations. The results for the FTF for the random and harmonic velocity modulations, are presented in Fig. 5. The FTF have been measured between 20 and 250 Hz, with a 5 Hz frequency resolution when harmonic modulations are considered. For random perturbations, data were collected and averaged over 600 windows of 4096 samples each. For both techniques, the sample frequency was fixed to 4096 Hz, which leads to a 1 Hz frequency resolution for the FTF measured with random disturbances.

The results collapse well with both methods of excitation and the random signal method is able to retrieve the main characteristics of the response of this conical flame. The FTF gain is

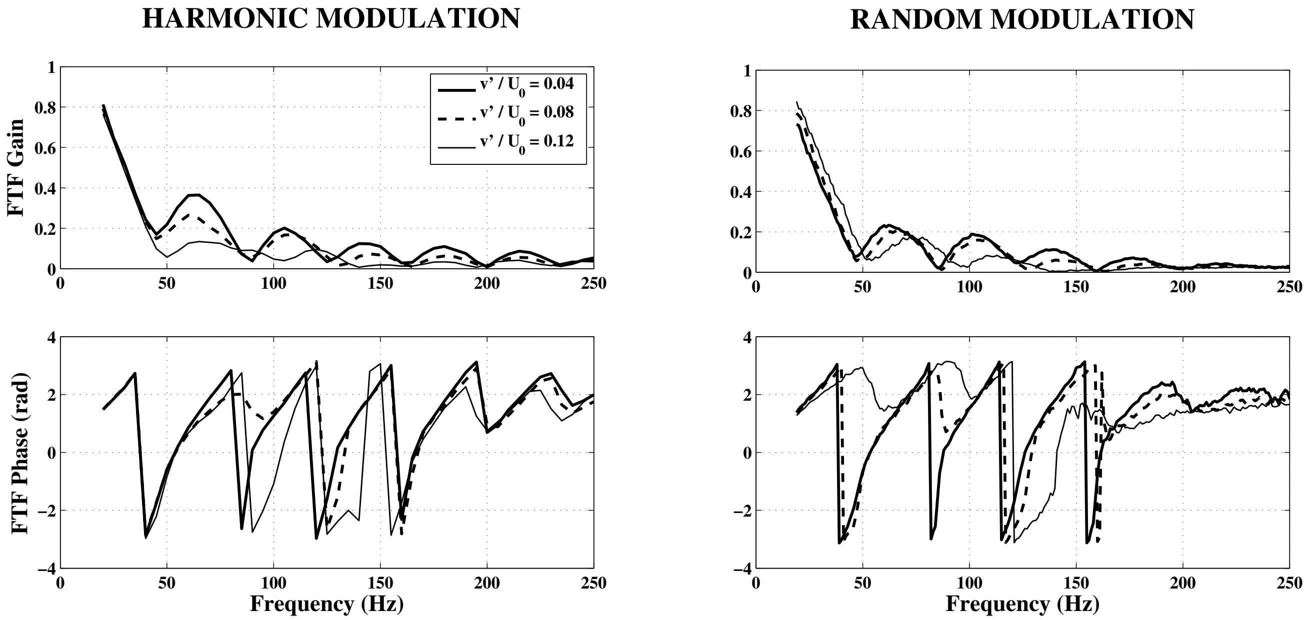

Figure 6. Gain and phase of the FTF obtained for different velocity perturbation levels. Left : results obtained with harmonic modulation. Right : results obtained with random disturbances.

well retrieved up to 45 Hz, where the flame response is strong. For higher excitation frequencies, the random modulation technique shows some differences on the gain, but it is still able to retrieve the global trend, as well as the position of the minima and maxima of the FTF gain. For the FTF phase, both methods give the same results. The random modulation technique, as well as the harmonic one, show that the phase increases linearly with the frequency up to about 200 Hz. This highlights the convective nature of the flame response, which then stops for higher frequencies while the phase reaches a constant value [20,24,25]. This saturation is well predicted by both techniques. This is in agreement with previous theoretical and experimental results on conical flame transfer functions, where the nearly constant slope of the phase can be linked with a convection time lag [8] while the saturation phenomenon observed at higher frequencies is still an ongoing issue. It is suspected that the latter is due to the contribution of the flame root dynamics to the FTF response. Most of the theoretical work conducted assumes a motionless flame root, while recent experiments indicate a significant response of the flame root [25] that may cause saturation of the phase at high forcing frequencies [20].

It is worth noticing that the harmonic modulation method took more than 30 mn to determine this response, with a 5 Hz frequency resolution, while the cross-correlation technique was carried out in 10 mn, with a 1 Hz frequency resolution. It represents a great overall improvement on the time and resolution. Overlap could also be used for the average cross-correlation technique, which again could divide by 2 (for a 50% overlap) the number of samples needed to reach statistical convergence of the method. Finally, this technique was used here on a specific configuration where the flame response vanishes for frequencies above 250 Hz. Some flames are known to features a higher frequency response. This would require about the same measurement time with the random modulation technique, but a considerable additional time to conduct all the experiments with harmonic modulations at higher forcing frequencies. Another advantage is that the better frequency resolution reduces significantly ambiguities about critical points of the FTF near maxima and minima for the gain and when the phase approaches π (modulo 2π) if no attempt is made to unwrap results. It is known that the FTF may feature different large and sudden changes in gain or phase. The alternative technique avoids having an a-priori knowledge of the FTF where these critical points are located and avoids refining the investigation in these regions.

Furthermore, SI tools were also tested to postprocess the data obtained with random broadband disturbances. The FTF gain and phase curves (not shown here) obtained with those tools perfectly fit the gain and phase curves obtained with averaged cross-correlation post-processing methods. The influence of the parameters on the convergence of the SI method will be further investigated in the section 4.

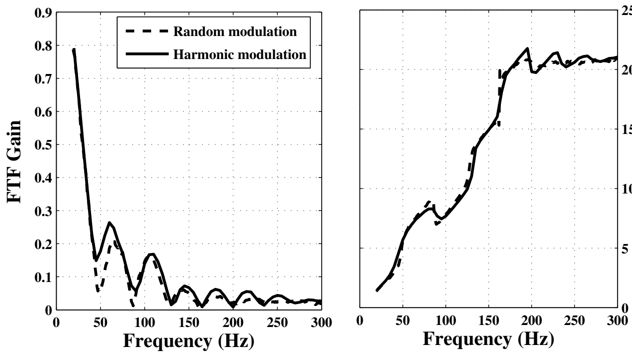

Figure 7. FTF obtained through harmonic and random velocity modulation and cross-correlation techniques, for a relative rms velocity perturbation of $v_{rms}/\bar{v} = 0.07$.

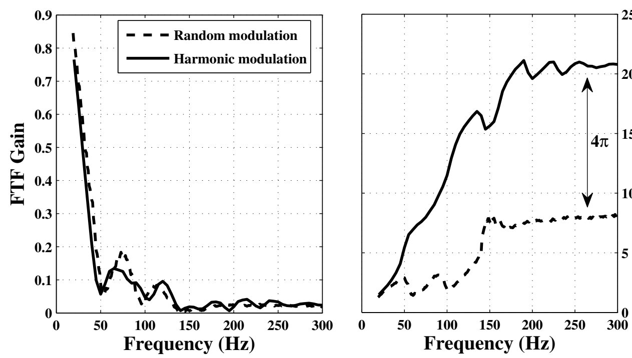

Figure 8. FTF obtained through harmonic and random velocity modulation and cross-correlation techniques, for a relative rms velocity perturbation of $v_{rms}/\bar{v} = 0.12$.

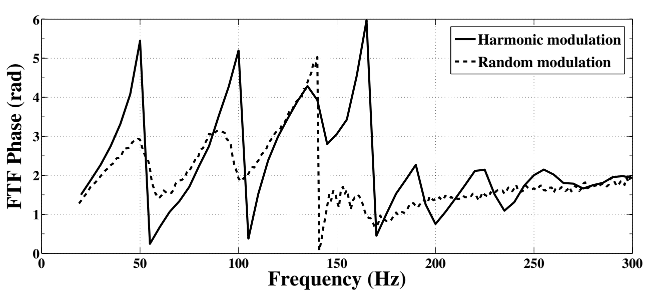

Figure 9. Flame Transfer Function Phases, wrapped between 0 and 2π, for a relative rms velocity perturbation of $v_{rms}/\bar{v} = 0.12$.

Modulation level effects

The methods previously described are known to work well for vanishingly small perturbations when the flame response remains linear. It is now interesting to examine effects of the perturbation amplitude. The FTF has been determined for different velocity fluctuation levels. Results for the same configuration $\bar{v} = 1.56$ m.s^{-1} and $\phi = 1.03$, are presented in Fig. 6. They are also compared with the the harmonic and random methods in Fig. 7, 8 and 10, respectively for relative rms velocity perturbations of about $v_{rms}/\bar{v} = 0.07$, 0.12 and 0.18.

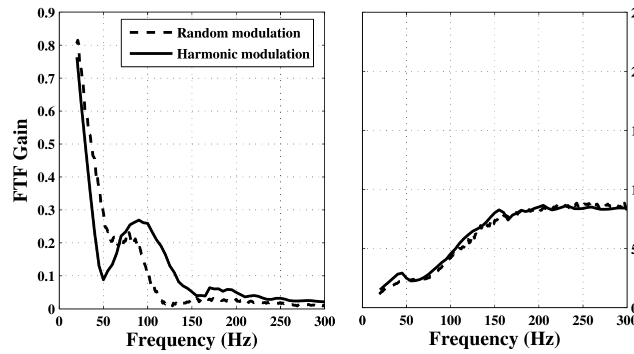

Figure 10. FTF obtained through harmonic and random velocity modulation and cross-correlation techniques, for a relative rms velocity perturbation of $v_{rms}/\bar{v} = 0.18$.

As indicated by the Fig. 6, both methods exhibit the same dependance of the FTF on the velocity perturbation level. A decreasing gain and an early saturation of the phase is observed, while the wrapped phase is weakly dependent on the perturbation amplitude at low frequencies. This is in agreement with previous experimental data obtained on the same type of configuration when submitted to increasing perturbation levels [24,25].

For a modulation level of $v_{rms}/\bar{v} = 0.07$, the comparison between both methods still shows a good agreement (Fig. 7). There are some differences in the FTF gain values, but the trends and extrema locations are still well retrieved. The FTF phase also exhibits a very good match. For a higher perturbation level $v_{rms}/\bar{v} = 0.12$, the results appeared to be less accurate. In Fig. 8, even though the gain curves are still close, the phase curves feature large differences, between 50 and 200 Hz. For larger frequencies, the phase saturation phenomenon is again retrieved with the two techniques, but at a different value for the phase. It is however found that these values match modulo 2π.

The main differences observed in the measurements essentially lie in the combined effects of the phase dependence to the perturbation level, and of unwrapping the phase across π where the phase is difficult to define precisely for small values of the gain. At intermediate forcing levels, the phase evolution may switch between a regular increase and a saturation with frequency. This behavior is very sensitive to the perturbation level. A small difference in the rms magnitude of the velocity perturbations between the harmonic and the random methods may trigger the transition between these two regimes at different frequencies. The phase evolution wrapped between 0 and 2π is presented in Fig. 9. This figure shows that the saturation frequency shifts from about 170 Hz for the harmonic modulation method to 140 Hz for the random modulation method. Outside of this frequency range, the trends and the saturation value are well retrieved.

For a perturbation level of $v_{rms}/\bar{v} = 0.18$, presented in Fig. 10, the gain is greatly underestimated by the random modulation technique between 50 and 150 Hz, while the phase curves still fit well between both measurements. It is however worth noticing that the slope of the phase curve takes a smaller value compared to measurements lade at a lower input level. It is explained by a shortening of the conical flame when submitted to large velocity perturbations. Reduction in the flame height induces a decrease of the average time lag for the perturbations to reach the flame surface. This in turn modifies the slope of the phase of the FTF.

These results clearly show the limits of the random modulation technique for large velocity disturbances. It is known that the flame response is non-linear. Using harmonic perturbations, the gain and the phase of the flame response are only analyzed at the forcing frequency. This yields the FTF in the first harmonic approximation while higher harmonics are discarded in this description. Measuring the FTF with random broadband velocity perturbations also includes the flame response at different harmonics. The FTF determined with this latter technique and examined at a certain frequency includes information on the non-linearity of the flame response at others frequencies.

This, along with the sensitivity of the phase to the velocity input level, explains the differences observed between results for the gain and the phase of the FTF obtained with the two techniques.

4 PARAMETER OPTIMIZATION

A sensitivity analysis is carried out in this section on the parameters of the SI method, to emphasize their importance on the determination of the FTF. As previously noticed, an important set of parameters to consider here is the number of forward and reverse filter coefficients n_a and n_b appearing in Eq. 6. In this study, n_a and n_b were chosen equal $n = n_a = n_b$. By increasing the number n, more samples in the time series are considered to build and IIF model of the system dynamics. This number must be chosen to capture the slowest time scale in the system studied. As a first approximation, it can be considered that this number is mainly linked to the largest time lag present in the flame response. Here, in the case of a conical flame, this time lag correspond to the time for a convective perturbation to travel from the base to the tip of the flame. It can be estimated by considering that the convective speed is the mean flow velocity :

$$\tau_{max} = \frac{H}{U_0} \tag{8}$$

where U_0 and H respectively stand for the mean flow velocity and the flame height. In the case presented here, $U_0 \approx 1.56$ m.s^{-1}, and $H \approx R/\tan\alpha$ where $R = 11$ mm is the burner radius and α the flame tip half-angle, defined for a steady conical flame by $\sin\alpha = S_L/U_0$. The minimum number of coefficients can be estimated : $n = \tau_{max}/\Delta t$ where Δt is the sampling time step. For a sampling frequency of 4096 Hz, this leads to a value of $n = 112$.

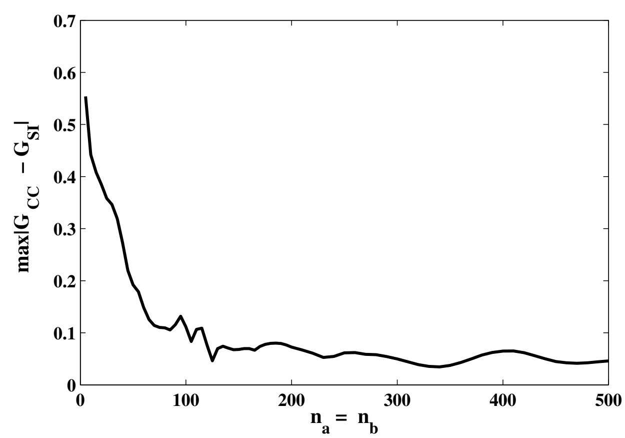

Figure 11. Convergence of the SI method : maximum error on the FTF gain plotted against the IIR filter order $n = n_a = n_b$.

A parametric study is conducted to analyze the effect of the number of coefficients n considered in the determination of the gain of the FTF with the SI method. The difference between the gain G_{SI} obtained with the SI method and the gain G_{CC} determined with the cross-correlation technique is calculated for the conical flame ($\bar{v} = 1.56$ m.s^{-1}, $\phi = 1.03$) submitted to random small velocity disturbances $v_{rms}/\bar{v} = 0.04$, all other parameters in the signal post-processing remaining identical. The results of these tests, shown in Fig. 11, demonstrate that the error computed for the FTF gain converges towards zero. Results do not improve for a number of coefficients larger than 125, indicating that the estimation of the minimum number of coefficient in Eq. 8 is a good approximation.

5 CONCLUSION

Different techniques to determine the flame transfer function to flow rate disturbances were examined and tested on a laminar conical flame. When random broadband excitation is considered, the flow modulation at the nozzle outlet must be characterized and controlled to obtain a white noise velocity perturbation signal instead of a colored signal filtered by the different electrical and mechanical elements in the actuation line. This broadband random velocity signal was then used to determine the FTF with averaged cross-correlation or system identification tools.

The results were compared to FTF measured with harmonic velocity modulations of the flow, where the modulation level was kept constant. The FTF gain and phase curves match well between the different methods for small amplitude perturbations. As the perturbation level amplitude is increased, the FTF gain is underestimated when random perturbation are considered. A general agreement is obtained for the phase evolution, even though the FTF phase features complex behaviors at low and high frequencies. The transition between these two regimes is very sensitive to the velocity perturbation level, which is the cause of the main differences observed.

A sensitivity analysis on the number of samples to consider in the SI technique was conducted. It emphasizes the link existing between the largest time lag of the flame response and the optimized SI parameters.

The method has to be further tested on a high-Reynolds-number flow in the future, but the same type of pre- and post-treatment is thought to be suited also for turbulent flows to separate incoherent disturbances induced by turbulence from coherent perturbations induced by the flow modulation.

ACKNOWLEDGMENT

The research leading to these results has received funding from the European Communitys Seventh Framework Programme (FP7/2007-2013) under Grant Agreement #ACP8-GA-2009-234009. This is part of the 4-year KIAI project started in May 2009, which is a European initiative financed under the FP7 and addresses innovative solutions for the development of new combustors in aero-engines. It aims at providing low NOx methodologies to be applied to design these combustors.

REFERENCES

[1] S. Candel. Combustion dynamics and control: Progress and challenges. *Proceedings of the Combustion Institute*, 29(1):1 – 28, 2002.

[2] S. Hubbard and A.P. Dowling. Acoustic instabilities in premix burners. In *AIAA Paper 98-2272*, 1998.

[3] W. Polifke, A. Poncet, C.O. Paschereit, and K. Doebbeling. Reconstruction of acoustic transfer matrices by instationary computational fluid dynamics. *Journal of Sound and Vibration*, 245(3):483 – 510, 2001.

[4] F. Nicoud, L. Benoit, C. Sensiau, and T. Poinsot. Acoustic Modes in Combustors with Complex Impedances and Multidimensional Active Flames. *AIAA Journal*, 45:426–441, 2007.

[5] L. Crocco and S. Cheng. Theory of combustion instability in liquid propellant rocket motors. In *AGARDO-GRAPH number 8*. Butterworths Science Publication, 1956.

[6] M. Fleifil, A. M. Annaswamy, Z. A. Ghoneim, and A. F. Ghoniem. Response of a laminar premixed flame to flow oscillations: A kinematic model and thermoacoustic instability results. *Combustion and Flame*, 106(4):487 – 510, 1996.

[7] S. Ducruix, D. Durox, and S. Candel. Theoretical and experimental determinations of the transfer function of a laminar premixed flame. *Proceedings of the Combustion Institute*, 28(1):765 – 773, 2000.

[8] T. Schuller, D. Durox, and S. Candel. A unified model for the prediction of laminar flame transfer functions: comparisons between conical and v-flame dynamics. *Combustion and Flame*, 134(1-2):21 – 34, 2003.

[9] T. Schuller, S. Ducruix, D. Durox, and S. Candel. Modeling tools for the prediction of premixed flame transfer functions. *Proceedings of the Combustion Institute*, 29(1):107 – 113, 2002.

[10] C.O. Paschereit, B. Schuermans, W. Polifke, and O. Mattson. Measurement of transfer matrices and source terms of premixed flames. *Journal of Engineering for Gas Turbines and Power*, 124(2):239–247, 2002.

[11] R. Balachandran, B.O. Ayoola, C.F. Kaminski, A.P. Dowling, and E. Mastorakos. Experimental investigation of the nonlinear response of turbulent premixed flames to imposed inlet velocity oscillations. *Combustion and Flame*, 143(1-2):37 – 55, 2005.

[12] K.T. Kim, J.G. Lee, H.J. Lee, B.D. Quay, and D.A. Santavicca. Characterization of forced flame response of swirl-stabilized turbulent lean-premixed flames in a gas turbine combustor. *Journal of Engineering for Gas Turbines and Power*, 132(4):041502, 2010.

[13] P.K. Baade. Design criteria and models for preventing combustion instabilities. *ASHRAE Transactions*, pages 449–465, 1978.

[14] T. Lieuwen and B.T. Zinn. The role of equivalence ratio oscillations in driving combustion instabilities in low nox gas turbines. *Symposium (International) on Combustion*, 27(2):1809 – 1816, 1998.

[15] P.L. Blackshear. Driving standing waves by heat addition. *Symposium (International) on Combustion*, 4(1):553 – 566, 1953.

[16] H.J. Merk. An analysis of unstable combustion of premixed gases. *Symposium (International) on Combustion*, 6(1):500 – 512, 1957.

[17] A.P. Dowling. A kinematic model of a ducted flame. *Journal of Fluid Mechanics*, 394(-1):51–72, 1999.

[18] W. Polifke and C. Lawn. On the low-frequency limit

of flame transfer functions. *Combustion and Flame*, 151(3):437 – 451, 2007.

[19] A.L. Birbaud, D. Durox, and S. Candel. Upstream flow dynamics of a laminar premixed conical flame submitted to acoustic modulations. *Combustion and Flame*, 146(3):541 – 552, 2006.

[20] V.N. Kornilov, K.R.A.M. Schreel, and L.P.H. de Goey. Experimental assessment of the acoustic response of laminar premixed bunsen flames. *Proceedings of the Combustion Institute*, 31(1):1239 – 1246, 2007.

[21] A. Bourehla and F. Baillot. Appearance and stability of a laminar conical premixed flame subjected to an acoustic perturbation. *Combustion and Flame*, 114(3-4):303 – 318, 1998.

[22] Preetham and T. Lieuwen. Nonlinear flame-flow transfer function calculations: Flow disturbance celerity effects. In *AIAA Paper 2004-4035*, 2004.

[23] T. Lieuwen. Nonlinear kinematic response of premixed flames to harmonic velocity disturbances. *Proceedings of the Combustion Institute*, 30(2):1725 – 1732, 2005.

[24] D. Durox, T. Schuller, N. Noiray, and S. Candel. Experimental analysis of nonlinear flame transfer functions for different flame geometries. *Proceedings of the Combustion Institute*, 32(1):1391 – 1398, 2009.

[25] N. Karimi, M.J. Brear, S-H. Jin, and J.P. Monty. Linear and non-linear forced response of a conical, ducted, laminar premixed flame. *Combustion and Flame*, 156(11):2201 – 2212, 2009.

[26] N. Noiray, D. Durox, T. Schuller, and S. Candel. A unified framework for nonlinear combustion instability analysis based on the flame describing function. *Journal of Fluid Mechanics*, 615(-1):139–167, 2008.

[27] L. Ljung. *System Identification : Theory for the user*. Prentice Hall, Englewood Cliffs, NJ, 2nd edition edition, 1999.

[28] A. Huber and W. Polifke. Dynamics of practical premixed flames, part i: model structure and identification. *International Journal of Spray and Combustion Dynamics*, 1(2):199–228, 2009.

[29] M. Zhu, A. P. Dowling, and K. N. C. Bray. Transfer function calculations for aeroengine combustion oscillations. *Journal of Engineering for Gas Turbines and Power*, 127(1):18–26, 2005.

[30] I. R. Hurle, R. B. Price, T. M. Sugden, and A. Thomas. Sound emission from open turbulent premixed flames. *Proceedings of the Royal Society of London. Series A. Mathematical and Physical Sciences*, 303(1475):409–427, 1968.

[31] Alan V. Oppenheim, Ronald W. Schafer, and John R. Buck. *Discrete-Time Signal Processing*. Prentice Hall, 2nd edition edition, 1998.

